Afyon Kocatepe Üniversitesi Fen ve Mühendislik Bilimleri Dergisi

Afyon Kocatepe University Journal of Science and Engineering

AKÜ FEMÜBİD **19** (2019) Özel Sayı (125-131) AKU J. Sci. Eng. **19** (2019) Special Issue (125-131)

# 2-Boyutlu $Ti_3C_2$ Tabakalarının İlaç Salım Potansiyelinin Belirlenmesi

**Derya KAPUSUZ**

*Gaziantep Üniversitesi, Mühendislik Fakültesi, Metalurji ve Malzeme Mühendisliği Bölümü, Gaziantep, Türkiye*

*e-posta: dkapusuz@gantep.edu.tr . ORCID ID: http://orcid.org/ 0000-0002-6935-9762*

Geliş Tarihi: 26.08.2019; Kabul Tarihi: 12.09.2019

***Anahtar kelimeler***
MXene; ilaç salınımı, 2-boyutlu; tabakalı; melatonin; ibuprofen

**Öz**

MXene'ler 2-boyutlu (2B) karbür/nitrür malzemelerin oluşturduğu geniş bir ailedir. Üçlü karbür fazlarının (MAX, M: geçiş elementi, A: A grup elementi, X: karbon ve/veya azot) tabakaları arasından A elementinin dağlanarak çıkarılması ile oluşturulurlar. MXene ailesi içinde en çok çalışılanlardan biri olan $Ti_3C_2T_x$ ($T_x$=-OH, -H, -F), grafen benzeri elektriksel performans ve kil benzeri tabakalı yapı göstermesi sayesinde grafen ve killerin avantajlı özellikleri birleştirmektedir. Grafene kıyasla, dağlama sonrası oluşan yüzey grupları ($T_x$) sayesinde yüzeyleri farklı şekillerde yapılandırılabilir ve daha geniş uygulama alanı sunabilirler. Akordeon morfolojisine sahip çoklu tabakalı (mL-) $Ti_3C_2$ parçacıkları kontrollü ilaç salımı için kullanılabilir. Parçacıkların ilaç salım potansiyellerini belirlemek için, mL-$Ti_3C_2$ tabakaları ibuprofen ve melatonin çözeltileri içinde farklı oranlarda dağıtılarak belirli sürelerde bekletilmiştir. Daha sonra filtrelenen çözeltilerden tabakaları arasına giren ilaç moleküllerinin tris-edta tampon çözeltisi içindeki salım davranışları araştırılmıştır. Sonuçlar ilacın tabakaları arasına girip 24 saate kadar aşamalı olarak salınabildiğini göstermiştir. Salım ortamının salım hızına etkisi belirgindir. Asidik ortamda salım daha yavaş gerçekleşmiştir. Bu çalışma, mL- $Ti_3C_2$ tabakalarının ilaç dağıtım uygulamalarında umut vaat edici malzemeler olduğunu göstermektedir.

# Investigation of Drug Release Potential of 2-Dimensional $Ti_3C_2$ Layers

***Keywords***
MXene; drug release; 2-dimensional; layered; melatonin; ibuprofen

**Abstract**

MXenes are a large family of 2-dimensional carbides/nitrides. They are derived from bulk ternary carbides, namely MAX phases (M: transition metal, A: A group element, X: carbon and/or nitrogen), through etching of A layers in between. $Ti_3C_2T_x$ ($T_x$=-OH, -H, -F), which is one of the most widely studied member of the family, could combine the advantageous properties of graphene and clays owing to its graphene-like electrical performance and clay-like layered structure. Compared to graphene, they offer a larger range of properties on account of their surface terminations ($T_x$) formed during or after etching. Using these surface terminations multilayered (mL-) $Ti_3C_2$ particles, possessing an accordion-like morphology might be used for controlled release of drugs. To investigate their drug release potential, mL- $Ti_3C_2$ layers were dispersed in ibuprofen and melatonin solutions at various concentrations for certain time intervals. Then solutions were filtered. Intercalated drug concentration and their release behavior in Tris-Edta buffer solution have been tested. Results indicated that drugs could be intercalated and released from mL- $Ti_3C_2$ layers up to 24 h. The influence of the release medium on controlling the release rate was remarkable. Release occurred slower in acidic media. This study showed that mL- $Ti_3C_2$ layers are promising materials for use in drug delivery applications.



14-16 Ekim 2019 tarihleri arasında düzenlenen X. Uluslararası Katılımlı Seramik Kongresi'nde sunulan bildirilerden seçilen çalışmadır.

## 1. Introduction

Layered materials are of special interest owing to their unique morphologies that allow for development of hybrid materials with controllable functionalities. Many researchers have stated the promising use of layered materials in biomedical and pharmaceutical research. It has been shown for many times that layered materials can intercalate and release drugs controllably if their structural properties are specifically optimized (Kitko *et al.* 2019; Shahabadi *et al.* 2018). Among various materials used in drug delivery literature, layered double hydroxides (LDHs) and graphene-based materials have been the leading materials owing to their superior properties including good biocompatibility, intercalation capability allowing for controlled release and/or conductivity, which is vital for sensor applications. Despite their advantageous properties and promising performance, each of these materials faced several challenges; essentially, degradation, uncontrolled release, lack of biocompatibility and conductivity (Kalaydina *et al.* 2018)

Considering these shortcomings, this work aimed to investigate the potential use of MXenes as drug reservoirs. Due to their layered morphology and water intercalative properties as clays and graphene-like conductivity, MXenes can act as - a bridge between clays and graphene - superior reservoirs for intercalation and release of drugs used in therapeutics and biosensing. Typically, MXenes are a large family of 2-dimensional layered carbides/nitrides derived by selective etching of A layer from well-known ternary carbides (MAX: M: transition metal, A: A group element, X: carbon and/or nitrogen) using chemical methods (Lin *et al.* 2018).

The drug intercalation and release behavior of MXenes from the interplanar spacing left by the etched Al ions were investigated using melatonin and ibuprofen as the model drugs and multilayered titanium carbide (mL-$Ti_3C_2$) - the most widely studied MXene – as the reservoir. Despite the fact that biocompatibility of $Ti_3C_2$ were revealed before (Lin *et al.* 2018), no study has been found in literature showing either MT or IBF release behavior of the MXenes.

Melatonin (MT; *N-acetyl-5-methoxytryptamine*) is an endogenous neurohormone and plays active role in various activities in the body, including neurogenesis, immunomodulation and immune defense, regulating circadian rhythms and inhibiting cancer growth. Orally administered MT has a short half-life (typically <40 min) (Roth *et al.* 2015). Therefore for controlled release, they have to be shielded and carried by some material. Similarly, one widely used nonsteroidal anti-inflammatory drug; ibuprofen (IBF; *p-isobutyl hydrotropic acid*) has also a short biological half-life (2 h) (Reis *et al.* 2013). Therefore MXenes are ideal candidates as strategic drugs to investigate the drug release potential of MXenes. The molecular structure of MT and IBF are shown in **Figure 1**.

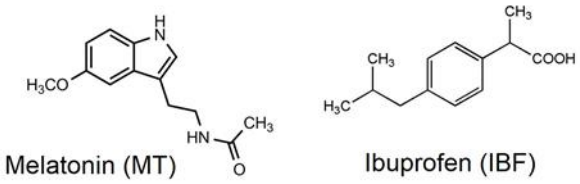


**Figure 1**. Chemical structure of MT and IBF.

## 2. Materials and Method

### *2.1 MXene Synthesis*

For the synthesis of mL-$Ti_3C_2$ particles, the well-known acid etching method was used. First, lithium fluoride (LiF, Sigma 449903) was dispersed in aqueous HCl (Sigma 320331, 6M). Then MAX Powders ($Ti_3AlC_2$) were added to this solution at 1:5 of MAX-to-molar ratio. Then, the solution was kept at 40 °C for 24 h under continuous stirring. After the etching reaction was completed, the solution was vacuum-filtered using a Buchner Funnel-glass flask filtering system. After the supernatant was filtered, the leftover precipitates were washed using first 500 mL ultrapure water, then 100 mL ethanol (99.9 %). After that, the powders on the filter paper were dried at 50 °C overnight.

### *2.2 MXene-Drug Hybrid Preparation*

IBF and MT were purchased from Sigma and used as-received. To prepare IBF and MT loaded mL-$Ti_3C_2$, first aqueous drug solutions were prepared at 21 µg/mL concentration, by dispersing them in fresh ultra-pure water. The solutions were stirred at room temperature (RT) for 1 h at 800 rpm. Then, certain amounts of mL-$Ti_3C_2$ powders were added to 10 mL of each drug solution. The formulation of hybrids are shown on **Table 1**. After stirring the hybrid solutions at RT for 24 h, the supernatant solutions were separated from particles and scanned by UV-Vis spectrophotometer.

### *2.3 Characterization and Testing*

To characterize the structure and morphology of mL-$Ti_3C_2$ particles, X-ray diffraction (XRD) and scanning electron microscopy (SEM) were used. For the XRD analysis, Rigaku D-Max-2200 diffractometer with Cu K-alpha radiation was used to scan the samples a 5-60° diffraction angles at a rate of 2°/min.

**Table 1**. mL-$Ti_3C_2$/ MT, IBF hybrid formulations

| Sample Code | mL-$Ti_3C_2$ (g) | Drug/DIW (µg/mL) Total vol.: 10 mL |
|---|---|---|
| IBF/MX-1 | 0.1 | 21 |
| IBF/MX-2 | 0.05 | |
| IBF/MX-3 | 0.025 | |
| MT/MX-1 | 0.1 | |
| MT/MX-2 | 0.05 | |
| MT/MX-3 | 0.025 | |

For morphological analysis, Nova Nano SEM 430 was used at 20 kV accelerating voltage. Before imaging, particles were coated with gold using high resolution sputter coater. UV-Vis spectroscopy (Shimadzu 1800) was used to investigate and compare the IBF/MT intercalation and release from mL-$Ti_3C_2$ layers after 24 h. Both IBF and MT had characteristic absorbance peaks centered at 222 nm and 280 nm, respectively (Qu *et al.* 2006, Girgin *et al.* 2016).

## 3. Results

### *3.1 Structural Analysis of mL-$Ti_3C_2$*

The XRD patterns and SEM images of $Ti_3AlC_2$ powders (before etching) and mL-$Ti_3C_2$ particles (after etching) are shown in **Figure 1** and **2**, respectively. The elemental composition of the mL-$Ti_3C_2$ powders were measured using SEM-EDS analysis and average of three EDS measurements was shown as inset in Figure 1.

Each peak in the XRD pattern of $Ti_3AlC_2$ particles could be ascribed to $Ti_3AlC_2$ (JCPDS: 01-074-8806). Typical diffraction peaks were present at 9.51°, 34.12°, 35.05°, 36.84°, 38.98°, 41.66°, 48.41° and could be ascribed to (002), (101), (102), (103), (104), (105) and (107) crystallographic planes, respectively. $Ti_3AlC_2$ is composed of Al layers, which are sandwiched between the octahedral $Ti_3C_2$ layers. The diffraction peaks of (00l) planes in the XRD pattern correspond to the presence of these octahedral layers (Jastrzebska *et al.* 2017)

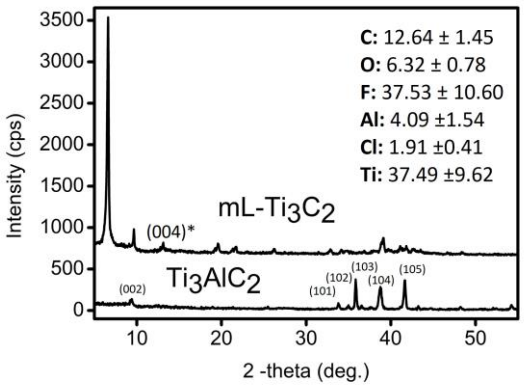


**Figure 1** a) XRD patterns and SEM images of b) $Ti_3AlC_2$ and c) mL-$Ti_3C_2$. Inset shows the weight percentages of O, F, Al, Cl and Ti in mL- $Ti_3C_2$ obtained by EDS measurements.

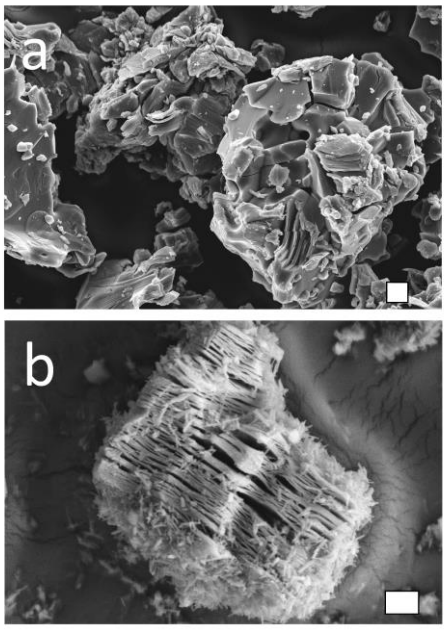


**Figure 2** SEM images of a) $Ti_3AlC_2$ and b) mL-$Ti_3C_2$ particles. Note that the length of each bar corresponds to 2 μm.

As Al layers in $Ti_3AlC_2$ were eliminated by etching, the interplanar (d-) spacing between $Ti_3C_2$ layers increases and it is reflected to the XRD pattern as a significant shifting of the (*00l*) peaks to smaller angles. In this work, the leaching out was revealed in XRD by the shifting of the (002) peak from 9.51° to 6.85° (demonstrated as *(002)**)

The comparison of XRD patterns before and after etching indicate that the Al ions were extracted out from the layers by LiF/HCl etching. This leaching out was revealed both by the shifting of the (002) peak from 9.51° to 6.85° (shown as (002)*) and the increased distance between layers in the SEM image compared to that of $Ti_3AlC_2$ as **Figure 2a** compared to **Figure 2b**. The 2.66° shifting of the (002) peak meant that the interplanar spacing between the (002) planes expanded by Al leaching out by adsorbed water layer going inside simultaneously. However, there was still some $Ti_3AlC_2$ unreacted, which was apparent from the tiny (002) peak in the XRD pattern of mL-$Ti_3C_2$, at its original position and also the 4.09 ± 1.54 wt. % Al content in EDS. In parallel with the literature, the mL-$Ti_3C_2$ particles could be coded as mL-$Ti_3C_2T_x$ as X denotes the surface terminations (OH, O, and F).

### *3.2 IBF and MT intercalation into mL-$Ti_3C_2$*

To investigate the IBF and MT intercalation capability of mL-$Ti_3C_2$ particles, three hybrid solutions were prepared at different mL-$Ti_3C_2$ concentrations (**Table 1**). Prior to analysis, to eliminate the by-products and/or unreacted $Ti_3AlC_2$, particles washed with DI water for 24 h, centrifuged and vacuum filtered with fresh ultrapure water until pH reaches 7 (pH equals 7 as impurities are cleared). Then particles were dried at 50 °C overnight.

The drug concentration and the total volume of drug solutions were kept constant at 21 μg/mL and 10 mL, respectively. In UV-Vis spectroscopy analyses of drug loading, the decreased absorbance of drug solution at its characteristic peak maxima correspond to adsorption/intercalation to MXenes from solution. In testing of drug release, vice versa. However, it was more complex than this simple reasoning that mL-$Ti_3C_2$ layers also released some by-products (i.e. surface terminations; $T_X$) to the solution. This release led to increase in UV absorbance in 200-350 nm range (Figure 3a, inset-MX). To eliminate the effect of this molecular release into the solution, the UV-Vis absorbance data of MX (control sample) was subtracted from that of each hybrid supernatant. In **Figure 3a**, the UV-Vis spectra of IBF/MX hybrid supernatants, from which the data of MX supernatant (Figure 3a, inset) was subtracted, are shown and compared to that of native aqueous IBF solution. The characteristic absorbance peak of IBF was at 222 nm when dissolved in ultra-pure water. However it shifted to higher wavelengths and broadened, indicating a possible interaction between IBF and MXene layers. The intensity of the peak maxima was highest in IBF/MX-1 which contained the highest amount of mL-$Ti_3C_2$, and decreased with decreasing mL-$Ti_3C_2$ content.

In **Figure 3b**, the UV-Vis absorbance curves of mL-$Ti_3C_2$ containing hybrid MT supernatant solutions are shown after subtraction of UV absorbance of mL-$Ti_3C_2$ and compared to that of native MT

solution. Native MT solution had two characteristic absorbance peaks centered at 233 nm and 280 nm. In this case, the absorbance of MT/MX supernatants was lower than the native solution. As the data of MX was subtracted, the curves revealed the pure effect of MT loading on MXene layers. Opposite to IBF/MX hybrids, as the mL-$Ti_3C_2$ content decreased the UV absorbance of the MT/MX hybrid supernatants at characteristic wavelengths (233/280 nm) decreased. Since the duration of exposing MXenes to drugs was identical in each case, then it could be stated that the MT absorbance increased with the decreasing MXene content in water. Whereas IBF intercalation decreased with increasing the MXene content. The absorbance decrease below 0 was due subtraction of the UV absorbance of unreacted mL-$Ti_3C_2$ particles.

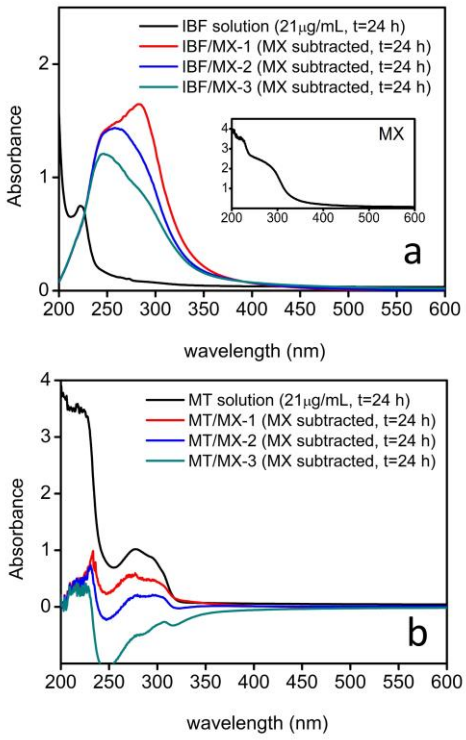


**Figure 3** UV-Vis absorbance spectra of a) IBF solutions b) MT solutions exposed to mL-$Ti_3C_2$ particles for 24 h, at different concentrations compared to native IBF and MT, respectively. Note that UV-Vis absorbance spectrum of mL-$Ti_3C_2$ *(inset) in (a))* was subtracted to eliminate the influence of by-products released from mL-$Ti_3C_2$ into water.

### *3.3 IBF and MT release from mL-$Ti_3C_2$ particles*

To investigate the IBF and MT release potential of MXenes, hybrid powders which were separated from the supernatants in Section 3.2 by filtering, were dispersed in Tris-Edta (TE, 10x) buffer at identical concentrations for 24 h.

In **Figure 4a**, the IBF release curves of hybrid particles are compared to UV-Vis absorbance curve of IBF-TE solution. In TE buffer, 21 µg IBF/mL solution revealed absorbance maximized at 218 nm and 233 nm, forming a wide absorbance band. Similar to the strategy for eliminating the effect of released by-products from MXenes in intercalation testing, the UV-Vis absorbance data of control MXene in TE buffer was subtracted from each data (identical to Figure 3a, inset). Since this was the measurement of release of the drug molecule to the solution, than the absorbance at the characteristic maxima was expected to increase by the release.

In Figure 4a, the data shows that the lowest absorbance was observed for IBF/MX- hybrid which indicated the highest MXene content. As the MXene amount in the hybrids decrease, the absorbance at the characteristic IBF peak increased.

To investigate the MT release behavior, same procedure was followed. Results are shown in **Figure 4b**. Native MT in TE buffer had only the characteristic absorbance maxima centered at 233 nm in TE buffer. The maxima at 280 nm disappeared. The hybrid containing the highest MXene also showed the peak at 233 nm but with much lower intensity.

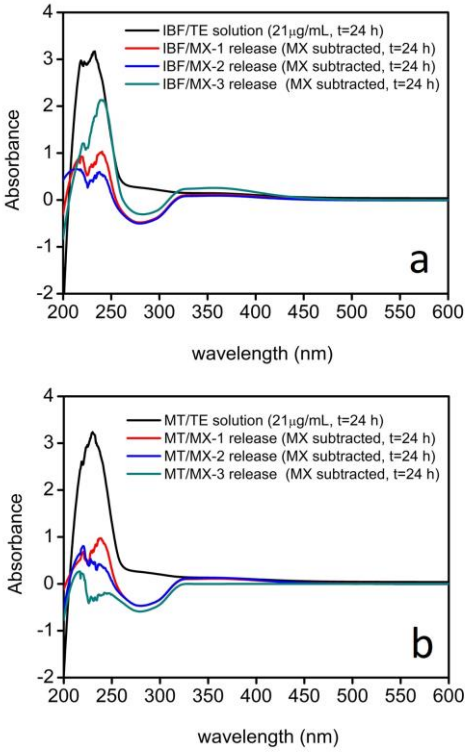


**Figure 4** UV-Vis absorbance spectra of a) IBF solutions b) MT solutions exposed to mL-$Ti_3C_2$ particles for 24 h, at different concentrations compared to native IBF and MT, respectively. Note that UV-Vis absorbance spectrum of mL-$Ti_3C_2$ *(inset) in (a))* was subtracted to eliminate the influence of by-products released from mL-$Ti_3C_2$ into water.

## 4. Discussion and Conclusion

In this work, the MT and IBF intercalation and release capabilities of mL-$Ti_3C_2$ particles were investigated for the first time in literature. For the intercalation test, both drugs were dissolved in ultrapure water at same concentration (21 µg/mL). IBF had a characteristic UV absorbance maxima at 222 nm. MT on the other hand, had this maxima at 280 nm with strong absorbance below 250 nm. Basically, the intercalation capability of particles could be revealed by shifting of the position and change in absorbance at these characteristic wavelengths after exposing the drug solutions to mL-$Ti_3C_2$ particles for 24 h. As the drug molecules were intercalated between the layers, the absorbance in the supernatant drug solution must have decreased due to intercalation. To eliminate the UV absorbance of surface terminations/by-products released from mL-$Ti_3C_2$ the UV absorbance curve was subtracted from each intercalation data.

In this manner, none of IBF solutions exposed to mL-$Ti_3C_2$ particles revealed absorbance maxima at its original position (222 nm). Probably the peak maxima shifted to higher wavelengths and absorbance was dominated by that in 250-350 nm range. During drug loading, the absorbance in 250-350 nm range decreased upon decreasing the MXene content. From here, it can only be concluded that an adsorption/intercalation reaction probably occurred between MXenes and IBF molecules. Examining the curves in Figure 4a revealed the release clearly. In TE buffer, presence of IBF in solution could be monitored by UV-Vis spectroscopy upon absorbance at 218 nm and 233 nm; the absorbance decreased upon decreasing the MXene content. It was revealed that higher amount of MXene led to higher amount of IBF release. As the pKa of IBF is 4.91 (Behera *et al.* 2012), and MXenes having negative surface charge it can be stated that IBF molecules were intercalated between the layers rather than adsorbed by the surface because of electrostatic repulsion around physiological pH (TE buffer, pH 7.5-8) The adsorption was blocked by the increased absorbance in 250-350 nm range but release could be directly observed in TE buffer.

Besides, the UV-Vis absorbance data given in Figure 3b revealed directly that MT could be adsorbed/intercalated into MXene layers. Relatively highest amount of MT loading was observed in MT/MX-3, which contained relatively the least amount of MXene. On the contrary, least amount of release was observed in MT/MX-3 pointing out that MT may chemically bond to MXene layers, thereby the release is not easy at short times. Only the molecules adsorbed by surface terminations could be released at first. In the overall, this work shows that MXene layers can be used as reservoirs for IBF and MT delivery. The MXene content and processing conditions (buffer/release medium acidity) must be optimized.

**Acknowledgement**

The Author acknowledges Prof. Dr. Michel W. Barsoum (*Dept. of Materials Science and Engineering, Drexel University, Philadelphia, PA/USA*) for providing the MAX powders and Gaziantep University Scientific Projects Governing Unit f(BAPYB) for funding the work under project number RM 16.01.

## 5. References

Behera, S.K., Oh, S.Y., Park, H.S. 2012. Sorptive removal of ibuprofen from water using selected soil minerals and activated carbon. *Int J Environ Sci Technol,* **9**, 85-94.

Girgin, B., Korkmaz, O., Yavaser, R., Karagozler, A.A. 2016. Production and drug release assesment of melatonin-loaded alginate/gum arabic beads. *JOTCSA,* **3(3),** 205-216.

Jastrzebska, A.M., Szuplewska, A., Wojciechowski, T., Chudy, M., Ziemkowska, W., Chlubny, L., Rozmyslowska, A., Olszyna, A. 2017. In vitro studies on cytotoxicity of Delaminated $Ti_3C_2$ MXene. *J Hazard Mater*, **339**, 1-8.

Kalaydina, V.R., Bajwa, K., Qorri, B., Decarlo, A., Szewczuk, M.R. 2018. Recent advances in "smart" delivery Systems for extended drug release in cancer therapy. *Int J NanoMed*, **13**, 4727-4745.

Kitko, K.E., Zhang, Q. 2019. Graphene-based nanomaterials: From production to integration with modern tools in neuroscience. *Frontiers in Systems Neuroscience*, **13(26)**, 1-17.

Lin, H., Chen, Y., Shi, J. 2018. Insights into 2D MXenes for versatile biomedical applications: Current advances and challenges ahead. *Advanced Science,* **5**, 201800518.

Qu, F., Zhu, G., Lin, H., Zhang, W., Sun, J., Li, S., Qiu, S. 2006. A controlled release of ibuprofen by systematically tailoring the Morphology of mesoporous silica materials. *J Solid State Chem*, **179**, 2027-2035.

Roth, T., Nir, T., Zisapel, N. 2015. Prolonged release melatonin for improving sleep in totally blind subjects: a pilot placebo-controlled multicenter trial. *Nature and Science of Sleep***, 7**, 13-23.

Shahabadi, N., Razinsari, M. 2018. Biological application of layered double hydroxides in drug delivery Systems*. J NanoAnalysis*, **5(4)**, 210-226.